


# Characteristics and potential use of residual waste from bauxite ore processing industry in West Kalimantan, Indonesia

Hendri Sutrisno<sup>1,2</sup>, Yulinah Trihadiningrum<sup>1\*</sup>, Januarti Jaya Ekaputri<sup>3</sup>,  
Fitriana Meilasari<sup>1,2</sup> , Adhi Yuniarto<sup>3</sup>

<sup>1</sup> Department of Environmental Engineering, Faculty of Civil, Planning, and Geo-Engineering, Institut Teknologi Sepuluh Nopember, Kampus ITS Sukolilo, Surabaya, 60111, Indonesia

<sup>2</sup> Department of Mining Engineering, Faculty of Engineering, Tanjungpura University, Pontianak, 78214, Indonesia

<sup>3</sup> Department of Civil Engineering, Faculty of Civil, Planning, and Geo-Engineering, Institut Teknologi Sepuluh Nopember, Kampus ITS Sukolilo, Surabaya, 60111, Indonesia

\* Corresponding author's e-mail: trihadiningrum@gmail.com

## ABSTRACT

Bauxite ore processing industry in West Kalimantan generates a voluminous waste that poses potential environmental risks due to its high pH and mineral contents. However, the substantial presence of calcium, silica, aluminum, and iron in the bauxite ore processing waste (BOPW) also presents opportunities for beneficial utilization. This study investigates the potential use of BOPW as liner material in municipal solid waste landfills, in order to minimize groundwater contamination risk. Physical, chemical, mineralogical, and environmental characteristics, which comprise water content, specific gravity, particle size, toxicity characteristic leaching procedure (TCLP), atterberg limit, compaction, consolidation were measured using relevant ASTM and USEPA methods. The results showed that the BOPW exhibited favorable properties as landfill liner. The low moisture content (20.35%), cohesiveness, and specific gravity of 2.94, low hydraulic conductivity ( $7.56 \times 10^{-7}$  cm/s) suggested suitability of the BOPW for landfill liner. Chemical analysis revealed predominant components of  $\text{Fe}_2\text{O}_3$ ,  $\text{Al}_2\text{O}_3$ ,  $\text{SiO}_2$ , and  $\text{Na}_2\text{O}$ , while mineralogical examination identified the presence of quartz, magnetite, hematite, and lime. The high pH value (11.93) supported chemical stability and immobilization of heavy metal contaminants. Despite favorable results of TCLP test, leachate quality analysis revealed elevated sodium concentrations (266 mg/L), which raised concerns about potential impact on surface water quality, particularly with the absence of specific regulatory standards. This study highlights BOPW's potential as a suitable landfill liner material, although further assessment for its long-term performance and application suitability is needed.

**Keywords:** bauxite processing waste, characteristics, landfill liner.

## INTRODUCTION

West Kalimantan has the largest bauxite mine in Indonesia, accounting for 66.77%, or 840 million tons of the total national reserve. The Tayan subdistrict in Sanggau Regency is one of the locations with the largest bauxite reserve (Ministry of EMR, 2016). Aluminum is produced using bauxite ore as the primary raw material. The refining process of bauxite ore into alumina involves the Bayer method (Al-Sakkari et al., 2022; Mukiza et al., 2019; Salim et al., 2023), sintering (Agrawal

and Dhawan, 2021; Amer, 2013), and a combination of both processes (Dubovikov and Jaskelainen, 2016).

Bauxite ore processing industry generates a fine, reddish-brown sludge residue (Manfroi et al., 2014; Shin et al., 2014). This sludge, locally named red mud, is termed as BOPW in this article. The high  $\text{Fe}_2\text{O}_3$  content causes the BOPW to have reddish color (Carneiro et al., 2018; IAI, 2015; Lingxiang et al., 2021; Lyu et al., 2021). The various bauxite sources influence the chemical composition of the BOPW, particularly in

the levels of  $\text{Al}_2\text{O}_3$ ,  $\text{SiO}_2$ ,  $\text{Fe}_2\text{O}_3$ ,  $\text{TiO}_2$ , and  $\text{Na}_2\text{O}$  (Nikbin et al., 2018). The Bayer process dominates the global alumina extraction method, accounting for approximately 90% of production (Gertsen, 2024; Lu et al., 2017; Tabereaux and Peterson, 2014). BOPW from the Bayer process has a higher iron content than that of sintering (Liu et al., 2014). Global annual generation of BOPW is estimated at 120 million tons (Power et al., 2011). About 1.5 to 1.6 tons of BOPW was generated as a byproduct for every ton of alumina production (Kaya and Soyer-Uzun, 2016).

BOPW exhibits high alkalinity, typically ranging from pH 10.5 to 12.5 (Shi et al., 2020; Wang et al., 2021; Wang et al., 2018). This is caused by the use of large amounts of caustic soda during the Bayer process (Shin et al., 2014). The high alkaline property makes the BOPW be classified as hazardous waste of corrosive category (Archambo and Kawatra, 2021; Zhang et al., 2018; Zhang et al., 2021). The high sodium and alkalinity contents in BOPW can potentially cause adverse environmental impacts to the environment (Díaz et al., 2015; Nikbin et al., 2018) and ecosystem damage if directly exposed (Stenchly et al., 2017; Winkler, 2014). It was also reported that the essential nature of BOPW could inhibit plant growth (Samal, 2021).

Environmental concerns which relate to improper bauxite mining waste handling has emerged recently in West Kalimantan. Public complaints arose from communities residing near bauxite mining operations. The BOPW was linked to the damage to *tengkawang* (*Shorea stenoptera*) and *durian* (*Durio kutajensis*) plantations in Melinau Regency (Anonymous, 2024). In a more recent incident, residents of Simpang Hilir Regency raised concerns about the water pollution of the Empawang River, a vital water source used by the community for bathing, sanitation, and washing. Additionally, local fishermen have reported the decline and death of fish population in this river (Anonymous, 2023). These cases highlight the potential environmental damage by the BOPW, as demonstrated by incidents worldwide. A leak at a BOPW storage facility in Hungary contaminated 1.000 hectares of land in 2010 (Gruiz et al., 2012; Mayes et al., 2011). In 2018 floods at a BOPW storage facility in Brazil caused soil contamination, which polluted water supplies with high levels of lead and aluminum (Alves, 2018). The BOPW has generally been disposed of in stockpiles (Balomenos et al., 2018).

Managing BOPW in stockpiles requires approximately 2% of the cost of alumina production (Wang et al., 2019). However, the BOPW has the potentials to be used as a source of iron for steel industry (Maihatchi et al., 2020), as raw material for cement and concrete production (Hou et al., 2021; Viyasun et al., 2021), for land reclamation in heavy metal-polluted areas (Hua et al., 2017; Lockwood et al., 2014; Zhou et al., 2017), as an adsorbent for heavy metal ions (Chen et al., 2019; Du et al., 2019; López-García et al., 2017; Pepper et al., 2018), and as a liner for acid mine drainage (Duchesne and Doye, 2005).

Indonesia faces a big challenge in municipal solid waste (MSW) management, with open dumping as the predominant method. Approximately 60% of landfills in Indonesia were still operated using the this method in 2021 (KLHK, 2021). Many landfills operation with this system was due to difficulties in obtaining cover soil (Kurniasari et al., 2014). Open dump landfill operation can cause soil and groundwater contamination (IEPA, 2024; Zhang et al., 2023). The environmental impact of landfills can be mitigated by implementing appropriate barrier layers, known as liners (Nath et al., 2023; Wan et al., 2023). Typical landfill liners include clay, geosynthetic clay liners (GCL), and composite layers. The later comprises compacted clay liners (CCL) and GCL (Emmanuel et al., 2020; Shu et al., 2019). The use of clay and artificial liners has several drawbacks, which particularly related to economics consideration and availability. Clay, a valuable resource with limited availability in Indonesia, has become a big challenge in landfill construction and operation despite its varying costs. Application of clay liners shows the widest cost range (US\$32.000–162.000 per hectare). In contrast, synthetic alternatives like geomembranes (US\$24.000–35.000 per hectare) and geocomposites (US\$33.000–44.000 per hectare) offer narrower cost ranges. The integration of these liner systems substantially increases the total landfill construction costs to US\$300.000–800.000 per hectare, depending on the combination of technologies employed. The significant cost variations in landfill cover construction necessitate careful material selection and design strategies to balance environmental sustainability with economic feasibility (Rubinos and Spagnoli, 2018). Therefore, a liner made from mine waste, including the BOPW, is an alternative substitute to clay (Rubinos et al., 2015). One of landfill liner requirements is having (K) of less

than  $1 \times 10^{-7}$  cm/s (USEPA, 1992b). Low K value can be achieved when sufficient fine particles fill the soil pores, and the absence of large particles hinders the process of compacting the soil into a dense mass (Benson and Othman, 1993).

Global industrial utilization of aluminium process waste remains limited, estimated at approximately 3% of annual generation (Evans, 2016). In Indonesia, large amounts of BOPW have not been used and are mostly haphazardly dumped. Therefore, BOPW quantity minimization is essential (Archambo & Kawatra, 2021). The BOPW can potentially be used as a primary MSW landfill liner material due to its fine particle size (average particle size  $< 10 \mu\text{m}$ ) (Rubinos and Barral, 2013) and high content of Si and Al (Maritsa et al., 2016). While previous studies investigated the potential of stored BOPW as landfill liner material (Fan et al., 2023; Kara et al., 2017; Rubinos and Spagnoli, 2018), this research was focused on the use of fresh BOPW from the Bayer process. Stored and fresh BOPW were reported to have different physical-chemical characteristics (Liu et al., 2007). Fresh BOPW, with its distinct chemical composition compared to stored BOPW, such as higher sodium content, may offer advantages in mitigating shrinkage issues commonly associated with BOPW layers. For this reason, this study, which aims to explore the characteristics and potential use of BOPW from West Kalimantan for landfill liner material, as a novel investigation.

At least there are 4 adjacent regencies to the bauxite mining in Tayan district, which urgently need cover material for landfill operation. These regencies, namely Sanggau, Kubu Raya, Sekadau, and Ketapang, still use open dump MSW landfill (Figure 1) method due to the inavailability of clay cover material. The current volume of dumped BOPW in the study area is approximately 396,600  $\text{m}^3$ . For this reason, this research. Results of this research are expected to provide a solution for BOPW management in the mining industry and a new alternative substitute for landfill liner.

## MATERIALS AND METHODS

### Sampling locations

The BOPW samples were obtained from the Indonesia Chemical Alumina mining company, which generated about 0.6 million metric tons of BOPW annually in Tayan Hilir District. The sampling site was located at coordinates  $0^{\circ}03'40.9''\text{S}$  and  $110^{\circ}08'38.4''\text{E}$  (Figure 2).

### Sample collection and preparation

About 150 kg fresh BOPW samples were collected using a shovel. The samples were homogenized using the shovel prior to analysis. Subsequently, the BOPW was dried in an oven at  $110^{\circ}\text{C}$  for 24 hours and then crushed. The resulting samples were sieved using a 200-mesh screen



**Figure 1.** Locations of BOPW stockpile, MSW landfills, and the adjacent regencies requiring landfill liner

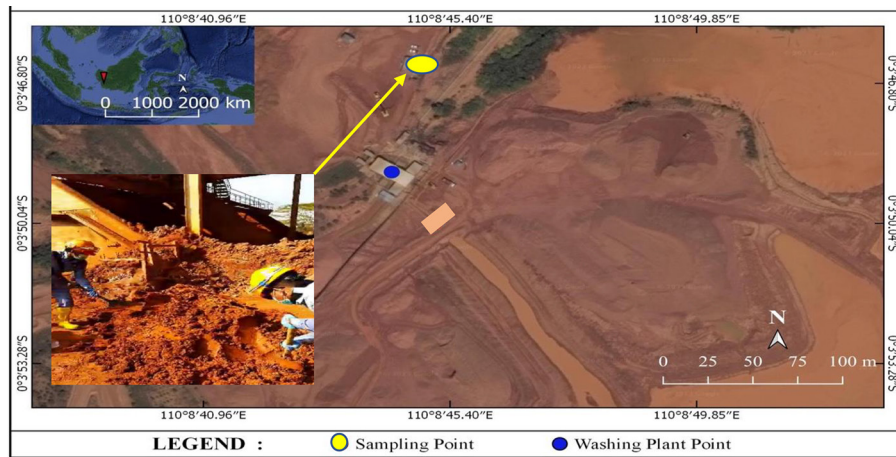


Figure 2. Sampling location

for thermogravimetric analysis (TGA), X-ray diffraction (XRD), and toxicity characteristic leaching procedure (TCLP) analyses. The samples that passed through a 325-mesh screen was specifically used for XRD analysis.

### Characterization of materials

#### Physical properties

The water content of the BOPW samples was determined according to ASTM D 2216-10, a standard test method for laboratory determination of water content of soil and rock. The moisture content was calculated using Equation 1.

$$\text{Water content} = \frac{\text{Weight of evaporated water}}{\text{Weight of dry sample}} \times 100\% \quad (1)$$

Determination of soil specific gravity ( $G_s$ ) was conducted following the standard test method for specific gravity of soil solids using a water pycnometer (ASTM D854-58). The specific gravity was calculated using Equation 2.

$$G_s = \frac{W_4}{(W_3 + W_4) - W_2} \quad (2)$$

where:  $W_1$  is weight of pycnometer and dry BOPW,  $W_2$  is weight of water, BOPW, and  $W_3$  is weight of pycnometer and distilled water, and  $W_4$  is dry weight of BOPW ( $W_1$  – the weight of empty pycnometer).

Particle size analysis of the BOPW was performed following standard test methods for particle-size distribution of soils using sieve analysis (ASTM D6913-04) and standard test method for amount of material in soil finer than

the No. 200 (75- $\mu\text{m}$ ) Sieve (ASTM D1140-14). Hydrometer analysis was conducted according to Standard test methods for particle-size distribution of fine-grained soils using the sedimentation analysis (ASTM D7928-16).

#### Chemical properties

The pH of the sample material was measured by mixing 1 g of sample with 5 mL of deionized water in a vial. The resulting mixture was agitated at 650 rpm in a shaker for 10 mins. The pH was then determined using a pH meter (Eutech pH 150). Chemical composition of the BOPW was determined using X-ray fluorescence (XRF) instrument. Mineral concentrations were expressed as % weights of  $\text{Fe}_2\text{O}_3$ ,  $\text{Al}_2\text{O}_3$ ,  $\text{SiO}_2$ ,  $\text{Na}_2\text{O}$ ,  $\text{TiO}_2$ ,  $\text{CaO}$ ,  $\text{SO}_3$ ,  $\text{K}_2\text{O}$ ,  $\text{MgO}$ ,  $\text{P}_2\text{O}_5$ ,  $\text{MnO}_2$ , and  $\text{Cr}_2\text{O}_3$ .

#### Crystal structure and mineral content

The mineralogical and crystal structure analyses of the BOPW sample were performed using XRD with K-alpha radiation ( $\lambda = 1.5406 \text{ \AA}$ ). The XRD data, collected over a  $2\theta$  range of  $10^\circ$  to  $90^\circ$ , were processed using Match software (versions 2 and 3) and the international centre for diffraction data (ICDD) database to identify mineral phases and their relative percentages.

#### Thermal analysis

The TGA was performed for characterizing the behavior change of the BOPW sample during heating and decomposition. The material mass was measured under controlled conditions during heating or cooling processes (Yao et al., 2022). The standard test for TGA analysis was based on

ASTM E1131-20 concerning standard test method for composition analysis by thermogravimetry. Sample heating process used Mettler Toledo TGA-DSC instrumentation and Huber CC 415 for cooling. Precisely 9.0405 mg sample was used for this analysis. The sample was heated from 25 °C to 1000 °C at a constant heating rate of 10 °C / min, which was maintained under a constant oxygen flow of 100 mL/min during the test.

#### Toxicity test

The TCLP test which determined whether a waste material is hazardous or not was applied using EPA Method 1311 (USEPA, 1992a). The results were compared to the regulatory quality standards according to Government Regulation of the Republic of Indonesia No. 22 Year 2021 concerning Environmental Protection and Management.

#### Geotechnical and hydraulic properties

Geotechnical characterization of the BOPW sample was conducted to assess its suitability as liner material. It included Atterberg limit tests comprising liquid limit (LL), plastic limit (PL), and (PI), compaction, and consolidation tests. Atterberg limits were determined according to ASTM D4318-17. Compaction tests were performed according to the Proctor method as specified by ASTM D698, while consolidation tests followed ASTM D2435. Consolidation data were used to establish the void ratio-log pressure relationship and calculate consolidation parameters. Consolidation parameters, including compression coefficient ( $C_c$ ), ( $C_s$ ), and coefficient of consolidation ( $C_v$ ), were determined using the approach outlined in Equation 3–4.

$$C_c = \frac{\Delta e}{\log \sigma_2 / \sigma_1} \quad (3)$$

$$C_s = \frac{\Delta e}{\log \sigma_1 / \sigma_2} \quad (4)$$

$$C_v = \frac{0,848 H^2}{t_{90}} \quad (5)$$

where:  $\Delta e$  represented the change in void ratio between initial and final states, and  $\sigma$  denoted the applied pressure in kg/cm<sup>2</sup>.

The swelling index was determined from the unloading portion of the consolidation test data. The time to achieve 90% consolidation ( $t_{90}$ ) was obtained from the Taylor's time-fitting method

applied to the consolidation curve, where  $H$  represented half the initial sample height.

Following proctor compaction, the hydraulic conductivity of the compacted BOPW was measured at the optimum moisture content using a rigid-wall falling-head permeameter. Distilled water was used as the permeant fluid. The hydraulic conductivity value was calculated using Equation 6 presented by Das et al. (1995).

$$K = \frac{aL \ln (h_1/h_2)}{At} \quad (6)$$

where:  $a$  represented the cross-sectional area of the vertical pipe (cm<sup>2</sup>),  $L$  denoted the specimen height (cm), and  $A$  denoted the cross-sectional area of the BOPW (cm<sup>2</sup>).  $h_1$  indicated the initial head (cm),  $h_2$  represented the head at time  $t$  (s), and  $k$  represented the hydraulic conductivity (cm/s).

## RESULTS AND DISCUSSION

### Physical properties

#### Moisture

The average moisture content of the BOPW material was 20.35% (Table 1). This value was lower than the previously reported ranges of 28% to 35.21% (Chen et al., 2023; Deelwal et al., 2014; Panda et al., 2017; Salih et al., 2020). This was likely due to the dewatering stage of the fresh BOPW prior to disposal. The process, which generally used a filter press equipment, could effectively reduced the moisture content in the BOPW to less than 35% (Hanumantha and Reddy, 2017)

Liner materials, even within the same classification, often exhibited significant variability in their initial moisture content, a factor which can profoundly impact their in-situ performance. Initial water content varied for each soil type. Clay soils generally exhibited moisture levels between 22.7% and 32.3% (Hamdi and Srasra, 2013; Wang et al., 2024). Silt soils fall within a range of 14% to 22.49% (Cheng et al., 2022; Du et al., 2023; Ma et al., 2023). In contrast to other materials, bentonite had a wider water content range, between 10.6% and 40% (El-Shamy et al., 2015; Muhmed et al., 2022; Zhang et al., 2022). Conversely, residual soil had a range of water content between 20.68 to 48.08% (Wibawa et al., 2018).

Water content affected the effectiveness of materials in the field of geotechnical engineering,

especially during the use of liners (Rowe, 2005). High water content can had a negative impact on liner performance. This was because water filled the pore space, which causes effective stress between soil particles, thereby increasing the permeability value of the material (Li et al., 2022). Additionally, fluctuations in water content caused significant volume changes that have an impacted on cracking and reduced the service life of the liner (Surbakti, 2021; Wulandari and Tjandra, 2019).

The low water content of the BOPW indicated its potential as a promising liner material. The water content of the BOPW was lower when compared to conventional liners that were commonly used. This allowed the BOPW to have a permeability value that was not much different from conventional liners. In addition, the BOPW also had the potential to have resistance to volume changes that can cause cracks. Variations in different water content values affected the physical and mechanical properties of materials such as shear strength, density and ability to absorb water. All three were properties that affected the effectiveness and long-term durability of the liner material. However, material with a high water content did not mean that it could not be used as a liner, this material can still be used if it went through a series of processing steps such as drying (Du et al., 2024; John et al., 2023; Salih et al., 2020).

*Particle size*

The results of the hydrometer analysis and particle size distribution test showed that the BOPW consisted of 29.98% clay, 52.13% silt and 17.89%

sand (Figure 3). Not less than 82.11% of the material passed the 200 mesh (0.075 mm) sieve, which was consistent with the research conducted by Chen et al., 2023 who reported a 55% pass rate of BOPW. Figure 4 (a-f) illustrates the BOPW particles retained on sieves #10, #20, #40, #100 and #200 and the fraction passing sieve #200. Permeability is the ability of a material to drain water. The permeability value is significantly influenced by the grain size of the material (Marschalko et al., 2021). The size of the material particles is directly proportional to their permeability value. This is because, when the particle size decreases, the pore space of the material shrinks and the flow path becomes more tortuous, resulting in decreased permeability (Lu et al., 2024; Marschalko et al., 2021; Zhang et al., 2020). The BOPW, dominated by clay and silt, indicates a low permeability value. This showed that the BOPW can be used for geotechnical applications.

The BOPW sample fell into the silty clay loam category according to the USDA soil texture classification system. This fine-grained soil typically exhibited cohesive properties (Hanumantha and Reddy, 2017; Kumar et al., 2023; Panda et al., 2017). The BOPW composition, characterized by a high proportion of both silt and clay, was expected to exhibit a fine texture, moderate water retention capacity, and a potential for drainage contingent upon the precise silt-clay ratio (Montelli et al., 2017; Zhang et al., 2021).

Despite its fine-grained texture, the BOPW exhibited a specific gravity of 2.77, which was notably higher than typically observed in clay

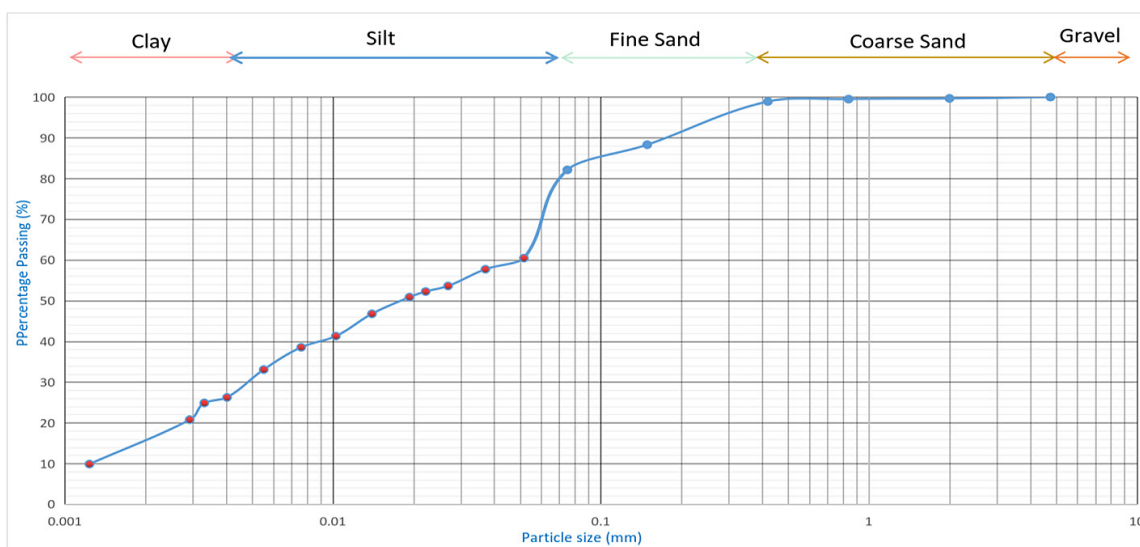


**Figure 3.** Distribution of particle sizes in BOPW

**Table 1.** Physical Properties of BOPW

Parameter	Value (%)
Gs	2.77
Water content	20.35
Maximum water content (Wc)	21.9
Size range (mm)	
0.001–0.0040	29.98
0.0041–0.075	52.13
0.076–2.0	17.89
2.1–4.76	0

soils. This value fell within the range of 2.7–3.45, as reported for similar materials (Chen et al., 2023; Kumar et al., 2023; Li et al., 2023). The presence of Fe oxides, particularly hematite and magnetite, within the BOPW matrix was likely responsible for this elevated specific gravity, as suggested by previous researchers (Hanumantha and Reddy, 2017; Salih et al., 2020).

### Chemical properties

#### *pH value*

The measured pH of BOPW was 11.93, consistent with previous reports indicated a pH range of 11–12 for similar materials (Khaerunisa et al., 2015; Santi, 2018). This value was significantly

higher than typical pH ranges observed in various soil types. Clay soils typically exhibited pH values between 4.5 and 7.5 (Bessaim et al., 2018; Momeni et al., 2022), while silt soils tended to have a neutral to slightly acidic pH, generally ranging from 6 to 7 (Al-Jabban et al., 2017). Residual soils demonstrated a wider range of pH values, influenced by the parent material and mineral composition (Foss and Segovia, 2020; Simon et al., 2021).

The pH value of a material could significantly influence its surface chemistry and, consequently, its interaction with polar molecules such as water. Materials that exhibited high pH values typically possessed a strong cation exchange capacity, suggesting that the BOPW, with its high pH, could potentially function as an adsorbent (Gray et al., 2016). The pH level significantly impacted the adsorption process. At low pH, the abundance of  $H_3O^+$  ions lead to competition between these ions and heavy metal cations for adsorption sites on the negatively charged surface. Conversely, under high pH conditions, the reduced concentration of  $H_3O^+$  ions facilitated the predominance of heavy metal ions in the adsorption process, primarily driven by electrostatic interactions (Al-Jabban et al., 2017). It is important to note that acidic soil pH can lead to increased soil permeability (Momeni et al., 2022), which may have implications for the material's performance as a liner or adsorbent.

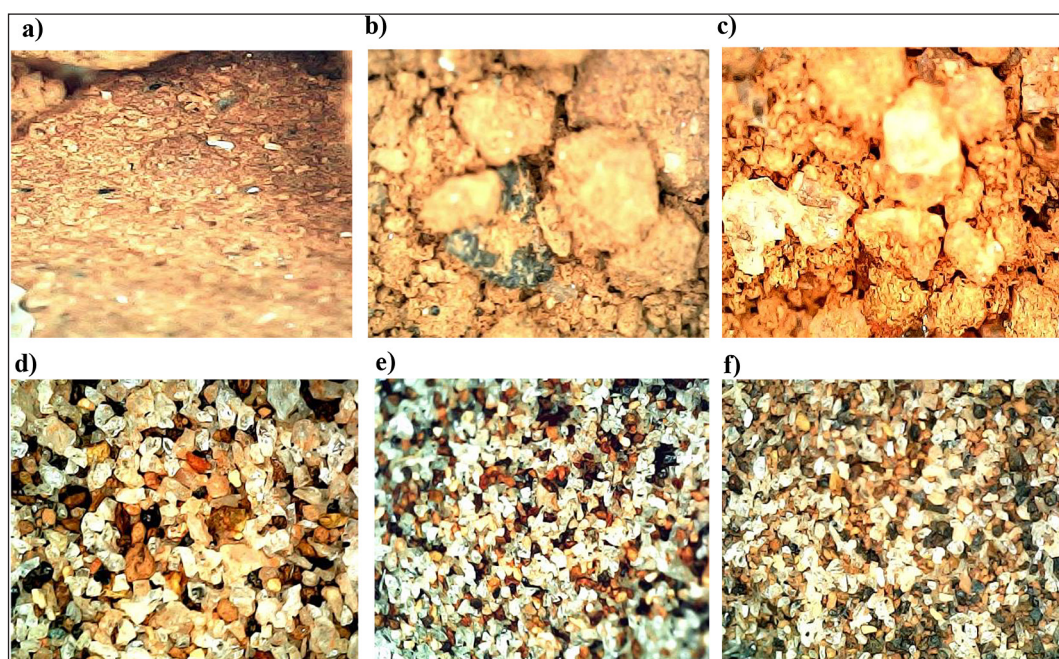


**Figure 4.** Photomicrographs of BOPW: (a) retained on sieve 10 mesh, (b) retained on sieve 20 mesh, (c) retained on sieve 40 mesh, (d) retained on sieve 100 mesh, (e) retained on sieve 200 mesh, (f) passed through a 200 mesh sieve, at 50 x magnifications

### Chemical composition

Results of XRF analysis revealed that the chemical composition of the primary component in BOPW dominated by  $\text{Al}_2\text{O}_3$ ,  $\text{SiO}_2$ ,  $\text{Fe}_2\text{O}_3$ , and  $\text{Na}_2\text{O}$  (Table 2). Microscopic imaging at 50x magnification showed white grains, indicative of excess sodium, while black grains were identified as metallic iron (Figure 4). The dominant reddish color of the BOPW indicated a high iron content. The chemical composition of the studied BOPW aligned with that reported for BOPW in China (Du et al., 2019; Hu et al., 2019; Lima et al., 2017). The high  $\text{Na}_2\text{O}$  content, a basic oxide, in the BOPW studied suggested a higher pH value compared to clay (Zhang et al., 2018).

The BOPW composition shared similarities with mineral composition of clay, which was typically dominated by  $\text{SiO}_2$  (46.40–85.51%) and  $\text{Al}_2\text{O}_3$  (2.96–39.63%) (Onyelowe et al., 2023; Purbasari and Samadhi, 2021) and  $\text{Al}_2\text{O}_3$  (2.96–39.63%) (Dewi et al., 2018, 2020). In contrast, residual soil was generally dominated by iron with a range of 52–75% (Silva et al., 2018); whereas Na-bentonite clay tended to have a higher silica content compared to its aluminum content (Kumar and Lingfa, 2020).

### Crystal structure and mineral content

Results of XRD analysis showed quartz, magnetite, hematite, and lime as the primary mineral

constituents of the investigated BOPW (Figure 5). Notably, gibbsite and boehmite, commonly found in other BOPW sources, were absent, indicating a distinct mineralogical composition (Li et al., 2023; Ramdhani et al., 2023; Wu and Liu, 2012). The high iron contents in BOPW were found in the form of hematite ( $\text{Fe}_2\text{O}_3$ ) and magnetite ( $\text{Fe}_3\text{O}_4$ ) (Liu et al., 2023; Sun et al., 2019). The high presence of silica was originated from its removal from bauxite ore during the Bayer process (Tabereaux and Peterson, 2014). Wu and Liu (2012) suggested that materials containing quartz could be used as adsorbents.

### Thermal stability and decomposition

The TGA analysis showed that exothermic process occurred at temperatures  $> 700\text{ }^\circ\text{C}$  over a period ranging from 69 to 96 min, peaking at  $716\text{ }^\circ\text{C}$  (Figure 6). Pre-dehydroxylation and hydroxylation processes occurred during the endothermic phase (Saukani et al., 2020; Waluyo et al., 2022). The endothermic process occurred at temperatures  $< 700\text{ }^\circ\text{C}$  over a period ranging from 0 to 68 min, peaking at  $265\text{ }^\circ\text{C}$ . This process took place within the temperature range of  $300\text{--}700\text{ }^\circ\text{C}$ . Organic materials underwent decomposition within the  $200\text{--}600\text{ }^\circ\text{C}$  temperature range (Wang et al., 2020). The percentage of material mass lost during combustion up to  $1000\text{ }^\circ\text{C}$  is 15.2%, which indicated that inorganic compounds dominate the

**Table 2.** Chemical composition of BOPW

Material	Parameters (% wt)												
	$\text{Al}_2\text{O}_3$	$\text{SiO}_2$	$\text{Fe}_2\text{O}_3$	CaO	$\text{Na}_2\text{O}$	$\text{TiO}_2$	MgO	$\text{K}_2\text{O}$	$\text{SO}_3$	$\text{P}_2\text{O}_5$	$\text{MnO}_2$	$\text{Cr}_2\text{O}_3$	LOI
BOPW	18.9	18.78	29.81	1.45	17.89	1.76	0.14	0.14	0.42	0.13	0.06	0.05	10.23

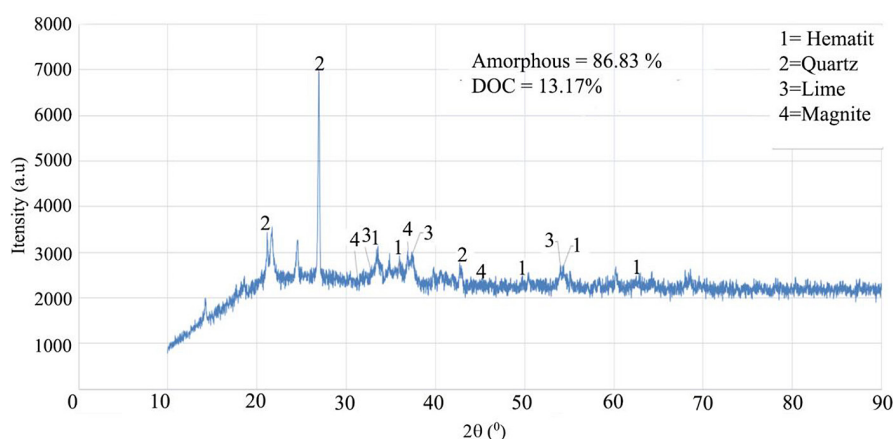


**Figure 5.** XRD analysis result of the BOPW



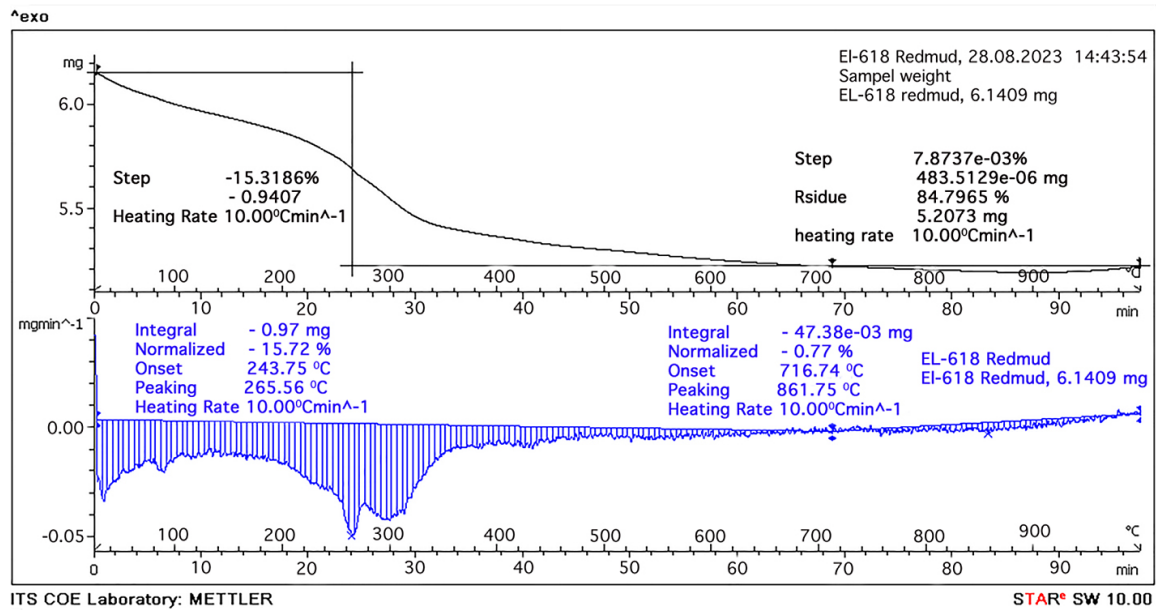


Figure 6. The TGA analysis curve of BOPW

BOPW material. Inorganic materials generally exhibit high surface area criteria, small pore sizes, and good hydrothermal stability, which made them a favorable choice for effective adsorption processes (Yeom and Kim, 2017; Zhang et al., 2015). Additionally, materials with high adsorption capacity were suitable for use as liners as they can reduce fluid movement and adsorb pollutants (Lakshmikantha and Sivapullaiah, 2006).

### Toxicity

Results of TCLP analysis of the BOPW material revealed that concentrations of inorganic parameters and anions were below Indonesian regulatory standards (Table 3). As iron is not specifically included in Indonesia's TCLP criteria, a conservative assessment was employed. This involved the use of drinking water quality standards for iron by multiplying a 100-fold safety factor as suggested by Intrakamhaeng et al. (2020). The results confirmed that heavy metal iron content was significantly lower than this limit.

### Geotechnical and hydraulic properties

The Atterberg limit test results revealed that the BOPW has a liquid limit of 29.25%, a plastic limit of 22.09%, and a plasticity index of 7.16% (Table 4). Based on these values, the unified soil classification system (USCS) categorizes the BOPW as clay mineral (inorganic silt) with

Table 3. TCLP test results

Parameter	Test result (mg/L)	Quality standards (mg/L)
Arsenic	< 0.003	0.5 **
Barium	0.21	35 **
Boron	< 0.10	25 **
Cadmium	< 0.06	0.15 **
Copper	< 0.06	10 **
Total Cyanide	< 0.03	3.5 **
Fluoride	1.8	75 **
Lead	< 0.07	0.5 **
Mercury	< 0.0003	0.05 **
Nitrate	4.0	2.500 **
Nitrite	< 0.03	150 **
Selenium	< 0.0003	0.5 **
Silver	< 0.10	5 **
Zinc	0.13	50 **
Antimony	< 0.10	1 **
Berilium	< 0.0027	0.5 **
Molibdenum	< 0.037	3.5 **
Nickel	< 0.10	3.5 **
Chromium hexavalent	0.33	2.5 **
Chloride	20.8	12.500 **
Iron	0.29	20 *
Iodide	< 0.04	5 **

**Note:** \*Indonesian Regulatory Drinking Water Quality Standards, Ministry of Health Regulation No.2 Years 2023 (This parameter is multiplied by 100), \*\*Regulatory Standards for Toxicity Characteristics through the TCLP in Indonesia, Government Regulation No. 22 Years 2021.

**Table 4.** Geotechnical and hydraulic properties

Parameter	Result	Unit
LL	29.25	%
PL	22.09	%
PI	7.16	%
SL	2.70	%
$\gamma_d$	1.68	g/cm <sup>3</sup>
n	0.39	
e	0.64	
K	$7.56 \times 10^{-7}$	cm/s

low plasticity. This classification aligns with previous research conducted in Spain (Rubinos et al., 2015). The calculated LL and PI values of BOPW exceed the minimum requirements (LL > 20 and PI > 7) to achieve a hydraulic conductivity of  $1 \times 10^{-7}$  cm/s (Benson and Othman, 1993; Daniel, 1993). While materials with PI > 30–40% generally exhibited higher shrinkage potential, and the BOPW with significantly lower PI value than 7%, indicated a lower shrinkage potential (Daniel, 1993). An activity ratio (PI/clay fraction) of 0.24, suggests that the BOPW can be classified as an inactive clay. This implied that the BOPW had a low tendency to swell or shrink (Skempton, 1953). Despite its low activity, the BOPW still had potential for use as a liner, provided it had a hydraulic conductivity value less than  $1 \times 10^{-7}$  cm/s. (Rubinos and Spagnoli, 2018; Wang et al., 2020).

The linear shrinkage of the BOPW was 2.7%. This value fell within the criteria range of BOPW from bauxite refineries of 1.5% to 4.2% (Rubinos et al., 2015; Wang and Liu, 2012). Shrinkage and plasticity were directly related properties influenced by factors such as particle size distribution, mineralogical composition (including mineral type and crystallinity), and the type of exchangeable cations present. The relatively low shrinkage value of the BOPW was attributed to the high sodium content, as sodium was known to mitigate shrinkage by reducing the material's sensitivity to moisture changes (Rubinos and Spagnoli, 2018). This low shrinkage potential was beneficial as it reduced the likelihood of cracking within the material.

Standard proctor compaction testing of the BOPW yielded a characteristic curve mirrored the behavior of clayey soils, where dry density increased with moisture content to a maximum value, followed by a decrease with further water

(Chaiyasat, 2019). A maximum dry unit weight ( $\gamma_d$ ) of 1.68 g/cm<sup>3</sup> was achieved at an optimum water content (Wc) of 21.9%. Compacting the raw material at its optimum moisture content produced a highly homogeneous and dense material. Analysis at the maximum dry weight revealed a porosity (n) of 0.391 and an associated void ratio (e) of 0.64. These parameters were found to exert an indirect influence to better infiltration characteristics of the material.

The measured BOPW hydraulic conductivity (K) was low  $7.56 \times 10^{-7}$  cm/s, which met the USEPA standards for liner applications of  $1 \times 10^{-7}$  cm/s. The low hydraulic conductivity is influenced by the inherent properties and particle size distribution of the soil. However, the base layer of landfills might deform shear due to the MSW weight burden, which potentially caused cracks in the liner. The load had the potential to damage the underlying protective layer, allowing leachate from the MSW heap to contaminate groundwater. The deformability of the landfill liner under MSW load was primarily governed by its compressibility.

Consistency tests of the BOPW resulted in a compression coefficient (Cc) of 0.078, a swelling coefficient (Cs) of 0.033, an initial void ratio (e) of 0.64, and a coefficient of consolidation (Cv) of  $2.27 \times 10^{-6}$  m<sup>2</sup>/s. The Cc value suggested moderate compressibility, implied that the liner will undergo a moderate degree of settlement under waste loading. This settlement can potentially enhance the liner's density, further reduced its permeability over time. However, it was crucial to ensure that the settlement did not induce cracking or discontinuities within the liner, which could compromise its integrity.

The low swelling coefficient of 0.033 indicates minimum expansion potential of the material when subjected to unloading or wetting. This characteristic was advantageous in coating material applications as it minimized the risk of cracking or significant volume changes due to moisture fluctuations or loading. The average consolidation coefficient (Cv) of  $2.27 \times 10^{-6}$  m<sup>2</sup>/s suggested a relatively slow consolidation rate. This slow consolidation rate was beneficial in landfill applications as it allows gradual adjustment to loads without the sudden cracking, although it may require longer construction times to achieve optimal compaction. The initial void ratio of 0.64, which decreased with increasing

**Table 5.** Post-consolidation hydraulic conductivity values

No	$\sigma$ (consolidation pressure) (kg/cm <sup>2</sup> )	$C_v$ (10 <sup>-3</sup> cm <sup>2</sup> /s)	$e$	$M_v$ (coefficient of volume compressibility) (cm <sup>2</sup> /kg)	$K$ (10 <sup>-7</sup> cm/s)	$C_v$ pairwise average (10 <sup>-3</sup> cm <sup>2</sup> /s)	$K_{\text{average}}$ (10 <sup>-7</sup> cm/s)
1	0.250	0.841	0.510				2.687
2	0.500	3.424	0.459	0.125	2.610	2.132	
3	1.000	3.502	0.403	0.067	1.502	3.463	
4	2.000	1.477	0.370	0.019	4.452	2.490	
5	4.000	2.496	0.347	0.007	1.600	1.986	
6	8.000	1.896	0.251	0.015	3.270	2.196	

load, indicated the potential for further compaction of the material under waste loads. This progressive compaction can enhanced the long-term effectiveness of the liner in preventing leachate seepage. The post-consolidation hydraulic conductivity of the material at each loading stage was determined based on the consolidation coefficient and volume compressibility coefficient obtained from consolidation testing. Analysis results indicated an average hydraulic conductivity of  $2.687 \times 10^{-7}$  cm/s (Table 5).

This low permeability is a highly desirable characteristic for landfill liner application, which met the typical regulatory requirement of less than  $1 \times 10^{-7}$  cm/s. Such low permeability effectively minimized leachate infiltration into the underlying soil, thus protecting groundwater resources from contamination. The consistency of hydraulic conductivity test results between the falling head method and consolidation test strengthened the validity of this study's findings.

Despite the low hydraulic conductivity of the BOPW, leachate analysis revealed the release of sodium and iron, reaching concentrations of 266 mg/L and 0.27 mg/L, respectively. Although the iron concentration did not yet reached the safe threshold for drinking water (0.3 mg/L according to Indonesian standards), the elevated sodium concentration in the leachate, reaching 266 mg/L, necessitates further investigation, eventhough specific regulatory standards for sodium in surface water have yet to be established. High sodium content can inhibit the performance of the leachate processing unit, so further research is needed. In addition to its potential as a landfill cover material, the BOPW is also able to absorb several heavy metals and dyes (Zhang et al., 2022). However, the effectiveness of its absorption is still unknown, so further research

is needed. Apart from that, economic feasibility also needs to be considered in the future.

## CONCLUSIONS

BOPW demonstrates significant potential as an alternative material for landfill liner. Based on its geotechnical and physicochemical characteristics, BOPW exhibits a hydraulic conductivity value that meets the requirements for use as a landfill liner. This finding provides opportunities for the mining industry to implement circular economy and clean industry principles by integrating BOPW into waste management infrastructure. Although this research yields promising results, the high sodium content requires attention. Given the significant sodium release observed in leachate analysis, and the lack of existing quality standards, comprehensive further research is crucial. Further research should investigate three key aspects: namely the potential impact of sodium release on wastewater treatment plant performance and the long-term performance of the BOPW liner. In addition, research on its economic feasibility analysis is also needed. Despite facing challenges, the potential of BOPW as a substitute for clay liners remains promising. Its utilization supports the principles of clean industry by reducing reliance on natural clay and mitigating environmental impact.

## Acknowledgements

The researchers gratefully acknowledge the Kurita Water and Environment Foundation, which supported this research with the KWEF Overseas Research Grant 2023 with Reference number 23Pid201. The authors also thank the Indonesia Chemical Alumina Company for providing the BOPW fresh samples

## REFERENCES

1. Agrawal, S., & Dhawan, N. (2021). Evaluation of red mud as a polymetallic source – A review. *Minerals Engineering*, 171, 107084. <https://doi.org/10.1016/j.mineng.2021.107084>
2. Al-Jabban, W., Knutsson, S., Laue, J., & Al-Ansari, N. (2017). Stabilization of clayey silt soil using small amounts of Petrit T. *Engineering*, 9(6), 540–562. <https://doi.org/10.4236/eng.2017.96034>
3. Al-Sakkari, E. G., O. Abdelmigeed, M., M. Naeem, M., & H. Dhawane, S. (2022). Inorganic wastes as heterogeneous catalysts for biodiesel production. In *Waste and Biodiesel* 137–163. Elsevier. <https://doi.org/10.1016/B978-0-12-823958-2.00010-0>
4. Alves, L. (2018). *Toxic water seeps from Norwegian mining site in Brazil's Amazon*. <https://riotimesonline.com/brazil-news/rio-politics/toxic-water-seeps-from-norwegian-mining-site-in-brazils-amazon/>
5. Amer, A. M. (2013). Hydrometallurgical processing of Egyptian bauxite [PDF]. *Physicochemical Problems of Mineral Processing*; 49; 431–442; ISSN 2084-4735. <https://doi.org/10.5277/PPMP130205>
6. Anonymous. (2023). Bauxite waste from PT. Brata Guna Perkasa's mine is suspected of contaminating the river. *Suarajournalist*. <https://www.suarajournalist-kpk.id/daerah/limbah-bauksit-tambang-ptbrata-guna-perkasa-diduga-mencemari-alur-air-sungai/>
7. Anonymous. (2024). Bauxite mining waste is causing problems for the people of Meliau. *Kalbarpost*. <https://kalbarpost.id/warga-meliau-keluhkan-lumpur-tambang-bauksit/>
8. Archambo, M., & Kawatra, S. K. (2021). Red mud: fundamentals and new avenues for utilization. *Mineral Processing and Extractive Metallurgy Review*, 42(7), 427–450. <https://doi.org/10.1080/08827508.2020.1781109>
9. ASTM D698. (2021). *Test Methods for Laboratory Compaction Characteristics of Soil Using Standard Effort (12,400 ft-lbf/ft<sup>3</sup> (600 kN-m/m<sup>3</sup>))*. ASTM International. <https://doi.org/10.1520/D0698-12R21>
10. ASTM D854-58. (2002). *Standard Test Methods for Specific Gravity of Soil Solids by Water Pycnometer*. ASTM International.
11. ASTM D1140-14. (2006). *Standard Test Methods for Determining the Amount of Material Finer than 75- $\mu$ m (No. 200) Sieve in Soils by Washing*. ASTM International.
12. ASTM D2435. (2011). *Test Methods for One-Dimensional Consolidation Properties of Soils Using Incremental Loading*. ASTM International. [https://doi.org/10.1520/D2435\\_D2435M-11R20](https://doi.org/10.1520/D2435_D2435M-11R20)
13. ASTM D4318-17. (2018). *Test Methods for Liquid Limit, Plastic Limit, and Plasticity Index of Soils*. ASTM International. <https://doi.org/10.1520/D4318-17E01>
14. ASTM D6913-04. (2009). *Standard Test Methods for Particle-Size Distribution of Soils Using Sieve Analysis*. ASTM International.
15. ASTM D7928-16. (2016). *Standard Test Method for Particle-Size Distribution (Gradation) of Fine-Grained Soils Using the Sedimentation (Hydrometer) Analysis*. ASTM International. <https://doi.org/10.1520/D7928-16>
16. Balomenos, E., Davris, P., Pontikes, Y., Panias, D., & Delipaltas, A. (2018). *Bauxite Residue Handling Practice and Valorisation Research in Aluminium of Greece*. 29–38. <https://doi.org/10.5281/zenodo.3587845>
17. Benson, C. H., & Othman, M. A. (1993). Hydraulic And mechanical characteristics of a compacted municipal solid waste compost. *Waste Management & Research*, 11(2), 127–142. <https://doi.org/10.1006/wmre.1993.1014>
18. Bessaim, M. M., Bessaim, A., Missoum, H., & Bendani, K. (2018). Effect of quick lime on physicochemical properties of clay soil. *MATEC Web of Conferences*, 149, 02065. <https://doi.org/10.1051/mateconf/201814902065>
19. Carneiro, J., Tobaldi, D. M., Hajjaji, W., Capela, M. N., Novais, R. M., Seabra, M. P., & Labrincha, J. A. (2018). Red mud as a substitute coloring agent for the hematite pigment. *Ceramics International*, 44(4), 4211–4219. <https://doi.org/10.1016/j.ceramint.2017.11.225>
20. Chaiyasat, S. (2019). Permeability of soil cement admixed with air foam. *IOP Conference Series: Materials Science and Engineering*, 652(1), 012022. <https://doi.org/10.1088/1757-899X/652/1/012022>
21. Chen, S., Jiang, J., Ou, X., & Tan, Z. (2023). Analysis of the synergistic effect on the strength characteristics of modified red mud-based stabilized soil. *Materials*, 16(18), 6104. <https://doi.org/10.3390/ma16186104>
22. Chen, S., Razaqpur, A. G., & Wang, T. (2023). Effects of a red mud mineralogical composition versus calcination on its pozzolanicity. *Construction and Building Materials*, 404, 133238. <https://doi.org/10.1016/j.conbuildmat.2023.133238>
23. Chen, X., Guo, Y., Ding, S., Zhang, H., Xia, F., Wang, J., & Zhou, M. (2019). Utilization of red mud in geopolymer-based pervious concrete with function of adsorption of heavy metal ions. *Journal of Cleaner Production*, 207, 789–800. <https://doi.org/10.1016/j.jclepro.2018.09.263>
24. Cheng, Y.-Y., Gao, X.-G., Liu, T.-H., Li, L.-X., Du, W., Hamad, A., & Wang, J.-P. (2022). Effect of water content on strength of alluvial silt in the lower Yellow River. *Water*, 14(20), 3231. <https://doi.org/10.3390/w14203231>

25. Daniel, D. E. (Ed.). (1993). *Geotechnical Practice for Waste Disposal*. Springer US. <https://doi.org/10.1007/978-1-4615-3070-1>
26. Deelwal, K., Dharavath, K., & Kulshreshtha, M. (2014). Evaluation of Characteristic properties of red mud for possible use as a geotechnical material in civil construction. *International Journal of Advances in Engineering & Technology*, 7(3), 1053–1059.
27. Dewi, R., Agusnar, H., Alfian, Z., & Tamrin. (2018). Characterization of technical kaolin using XRF, SEM, XRD, FTIR and its potentials as industrial raw materials. *Journal of Physics: Conference Series*, 1116, 042010. <https://doi.org/10.1088/1742-6596/1116/4/042010>
28. Dewi, R., Agusnar, H., Alfian, Z., & Tamrin. (2020). Physicochemical characterization of natural kaolin from Jaboi Indonesia. *Rasayan Journal of Chemistry*, 13(01), 382–388. <https://doi.org/10.31788/RJC.2020.1315523>
29. Diaz, B., Freire, L., Nóvoa, X. R., & Pérez, M. C. (2015). Chloride and CO<sub>2</sub> transport in cement paste containing red mud. *Cement and Concrete Composites*, 62, 178–186. <https://doi.org/10.1016/j.cemconcomp.2015.02.011>
30. Du, C., Lu, X., & Yi, F. (2024). Impact of modifiers on soil–water characteristics of graphite tailings. *Scientific Reports*, 14(1), 4186. <https://doi.org/10.1038/s41598-024-52826-6>
31. Du, Y., Dai, M., Cao, J., & Peng, C. (2019). Fabrication of a low-cost adsorbent supported zero-valent iron by using red mud for removing Pb(II) and Cr(VI) from aqueous solutions. *RSC Advances*, 9(57), 33486–33496. <https://doi.org/10.1039/C9RA06978J>
32. Du, Z., Zhang, Z., Wang, L., Zhang, J., & Li, Y. (2023). Effect of moisture content on the permanent strain of yellow river alluvial silt under long-term cyclic loading. *Sustainability*, 15(17), 13155. <https://doi.org/10.3390/su151713155>
33. Dubovikov, O. A., & Jaskelainen, E. E. (2016). Processing of low-quality bauxite feedstock by thermochemistry-bayer method. *Journal of Mining Institute*, 221, 668–674. <https://doi.org/10.18454/PMI.2016.5.668>
34. Duchesne, J., & Doye, I. (2005). Effectiveness of covers and liners made of red mud bauxite and/or cement kiln dust for limiting acid mine drainage. *Journal of Environmental Engineering*, 131(8), 1230–1235. [https://doi.org/10.1061/\(ASCE\)0733-9372\(2005\)131:8\(1230\)](https://doi.org/10.1061/(ASCE)0733-9372(2005)131:8(1230))
35. El-Shamy, A. M., Shehata, M. F., & Ismail, A. I. M. (2015). Effect of moisture contents of bentonitic clay on the corrosion behavior of steel pipelines. *Applied Clay Science*, 114, 461–466. <https://doi.org/10.1016/j.clay.2015.06.041>
36. Emmanuel, E., Anggraini, V., Raghunandan, M. E., & Asadi, A. (2020). Utilization of marine clay as a bottom liner material in engineered landfills. *Journal of Environmental Chemical Engineering*, 8(4), 104048. <https://doi.org/10.1016/j.jece.2020.104048>
37. Evans, K. (2016). The History, Challenges, and New Developments in the Management and Use of Bauxite Residue. *Journal of Sustainable Metallurgy*, 2(4), 316–331. <https://doi.org/10.1007/s40831-016-0060-x>
38. Fan, J., Yan, J., Zhou, M., Xu, Y., Lu, Y., Duan, P., Zhu, Y., Zhang, Z., Li, W., Wang, A., & Sun, D. (2023). Heavy metals immobilization of ternary geopolymer based on nickel slag, lithium slag and metakaolin. *Journal of Hazardous Materials*, 453, 131380. <https://doi.org/10.1016/j.jhazmat.2023.131380>
39. Foss, J. E., & Segovia, A. V. (2020). Rates of soil formation. In R. G. LaFleur (Ed.), *Groundwater as a Geomorphic Agent* (1st ed., 1–17). Routledge. <https://doi.org/10.4324/9781003028833-1>
40. Gertsen, A. (2024, January 17). *Aluminium Production*. [https://www.aluminiumleader.com/production/how\\_aluminium\\_is\\_produced/](https://www.aluminiumleader.com/production/how_aluminium_is_produced/)
41. Government of the Republic of Indonesia. (2021). *Government Regulation No. 22 of 2021 concerning Environmental Protection and Management* (22).
42. Gray, N., Lumsdon, D. G., & Hillier, S. (2016). Effect of pH on the cation exchange capacity of some halloysite nanotubes. *Clay Minerals*, 51(3), 373–383. <https://doi.org/10.1180/claymin.2016.051.3.04>
43. Gruiz, K., Feigl, V., Klebercz, O., Anton, A., & Vaszita, E. (2012). Environmental risk assessment of red mud contaminated land in Hungary. *GeoCongress 2012*, 4156–4165. <https://doi.org/10.1061/9780784412121.427>
44. Hamdi, N., & Srasra, E. (2013). Hydraulic conductivity study of compacted clay soils used as landfill liners for an acidic waste. *Waste Management*, 33(1), 60–66. <https://doi.org/10.1016/j.wasman.2012.08.012>
45. Hanumantha, R., & Gangadhara Reddy, N. (2017). Zeta Potential and Particle Size Characteristics of Red Mud Waste. In G.L. Sivakumar, K. R. Reddy, A. De, & M. Datta (Eds.), *Geoenvironmental Practices and Sustainability* (pp. 69–89). Springer Singapore. [https://doi.org/10.1007/978-981-10-4077-1\\_8](https://doi.org/10.1007/978-981-10-4077-1_8)
46. Hou, D., Wu, D., Wang, X., Gao, S., Yu, R., Li, M., Wang, P., & Wang, Y. (2021). Sustainable use of red mud in ultra-high performance concrete (UHPC): Design and performance evaluation. *Cement and Concrete Composites*, 115, 103862. <https://doi.org/10.1016/j.cemconcomp.2020.103862>
47. Hu, Y., Liang, S., Yang, J., Chen, Y., Ye, N., Ke, Y., Tao, S., Xiao, K., Hu, J., Hou, H., Fan, W., Zhu, S., Zhang, Y., & Xiao, B. (2019). Role of Fe species in geopolymer synthesized from alkali-thermal

- pretreated Fe-rich Bayer red mud. *Construction and Building Materials*, 200, 398–407. <https://doi.org/10.1016/j.conbuildmat.2018.12.122>
48. Hua, Y., Heal, K. V., & Friesl-Hanl, W. (2017). The use of red mud as an immobiliser for metal/metalloid-contaminated soil: A review. *Journal of Hazardous Materials*, 325, 17–30. <https://doi.org/10.1016/j.jhazmat.2016.11.073>
49. IAI. (2015). *Bauxite Residue Management: Best Practice*. International Aluminium Institute.
50. IEPA. (2024). *Waste management Open Dumping*. <https://epa.illinois.gov/topics/waste-management/illegal-dumping/open-dumping.html>
51. Intrakamhaeng, V., Clavier, K. A., & Townsend, T. G. (2020). Hazardous waste characterization implications of updating the toxicity characteristic list. *Journal of Hazardous Materials*, 383, 121171. <https://doi.org/10.1016/j.jhazmat.2019.121171>
52. John, N., Fathima, P. S., Harsha, V. S., Paul, N. M., & Nisha, P. (2023). Physical Conversion of Biomass: Dewatering, Drying, Size Reduction, Densification, and Separation. In S. Thomas, M. Hosur, D. Pasquini, & C. Jose Chirayil (Eds.), *Handbook of Biomass* (pp. 1–28). Springer Nature Singapore. [https://doi.org/10.1007/978-981-19-6772-6\\_37-1](https://doi.org/10.1007/978-981-19-6772-6_37-1)
53. Kara, İ., Yilmazer, D., & Akar, S. T. (2017). Metakaolin based geopolymer as an effective adsorbent for adsorption of zinc(II) and nickel(II) ions from aqueous solutions. *Applied Clay Science*, 139, 54–63. <https://doi.org/10.1016/j.clay.2017.01.008>
54. Kaya, K., & Soyer-Uzun, S. (2016). Evolution of structural characteristics and compressive strength in red mud–metakaolin based geopolymer systems. *Ceramics International*, 42(6), 7406–7413. <https://doi.org/10.1016/j.ceramint.2016.01.144>
55. Khaerunisa, H., Setiawan, W. A., Damayanti, R., Surono, W., Astika, H., & Lutfi, M. (2015). *Processing and Utilization of Bauxite Residue (Red Mud) for Peat Amendment and Acid Mine Drainage Neutralization*. Puslitbang Teknologi Mineral dan Batubara.
56. KLHK. (2021). *Performance Report of the Directorate General of Waste Management 2021*. Directorate General of Waste Management, Toxic Waste and Hazardous Materials, Ministry of Environment and Forestry. <https://drive.google.com/file/d/1qcfgtVnWNHj7TepIkIr3lsoLujSI44Z/view>
57. Kumar, A., & Lingfa, P. (2020). Sodium bentonite and kaolin clays: Comparative study on their FT-IR, XRF, and XRD. *Materials Today: Proceedings*, 22, 737–742. <https://doi.org/10.1016/j.matpr.2019.10.037>
58. Kumar, S. N., Sinha, A. K., & Madan, S. K. (2023). Characterisation of stabilised red mud waste material for road infrastructure. *Materials Today: Proceedings*, 93, 41–46. <https://doi.org/10.1016/j.matpr.2023.06.229>
59. Kurniasari, O., Damanhuri, E., Padmi, T., & Kardeana, E. (2014). Landfill Cover Soil Uses Old Waste as a Methane Oxide Media to Reduce Methane Gas Emissions. *Bumi Lestari*, 14(1), 46–52.
60. Lakshmikantha, H., & Sivapullaiah, P. V. (2006). Relative performance of lime stabilized amended clay liners in different pore fluids. *Geotechnical and Geological Engineering*, 24(5), 1425–1448. <https://doi.org/10.1007/s10706-005-0886-7>
61. Li, C., Nie, B., Feng, Z., Wang, Q., Yao, H., & Cheng, C. (2022). Experimental Study of the Influence of Moisture Content on the Pore Structure and Permeability of Anthracite Treated by Liquid Nitrogen Freeze–Thaw. *ACS Omega*, 7(9), 7777–7790. <https://doi.org/10.1021/acsomega.1c06631>
62. Li, X.-F., Zhang, T.-A., Lv, G.-Z., Wang, K., & Wang, S. (2023). Summary of Research Progress on Metallurgical Utilization Technology of Red Mud. *Minerals*, 13(6), 737. <https://doi.org/10.3390/min13060737>
63. Lima, M. S. S., Thives, L. P., Haritonovs, V., & Bajars, K. (2017). Red mud application in construction industry: *Review of benefits and possibilities*. *IOP Conference Series: Materials Science and Engineering*, 251, 012033. <https://doi.org/10.1088/1757-899X/251/1/012033>
64. Lingxiang, H., Chunlei, L., Haibin, W., Xingxing, L., Yongrong, Q., & Xuechen, Z. (2021). Research Progress on Comprehensive Utilization of Red Mud. *Journal of Physics: Conference Series*, 2009(1), 012021. <https://doi.org/10.1088/1742-6596/2009/1/012021>
65. Liu, W., Chen, X., Li, W., Yu, Y., & Yan, K. (2014). Environmental assessment, management and utilization of red mud in China. *Journal of Cleaner Production*, 84, 606–610. <https://doi.org/10.1016/j.jclepro.2014.06.080>
66. Liu, Y., Lin, C., & Wu, Y. (2007). Characterization of red mud derived from a combined Bayer Process and bauxite calcination method. *Journal of Hazardous Materials*, 146(1–2), 255–261. <https://doi.org/10.1016/j.jhazmat.2006.12.015>
67. Liu, Y., Zhuge, Y., Chen, X., Duan, W., Fan, R., Outhred, L., & Wang, L. (2023). Micro-chemo-mechanical properties of red mud binder and its effect on concrete. *Composites Part B: Engineering*, 258, 110688. <https://doi.org/10.1016/j.compositesb.2023.110688>
68. Lockwood, C. L., Mortimer, R. J. G., Stewart, D. I., Mayes, W. M., Peacock, C. L., Polya, D. A., Lythgoe, P. R., Lehoux, A. P., Gruiz, K., & Burke, I. T. (2014). Mobilisation of arsenic from bauxite residue (red mud) affected soils: Effect of pH and redox conditions. *Applied Geochemistry*, 51, 268–277. <https://doi.org/10.1016/j.apgeochem.2014.10.009>

69. López-García, M., Martínez-Cabanas, M., Vilariño, T., Lodeiro, P., Rodríguez-Barro, P., Herrero, R., & Barriada, J. L. (2017). New polymeric/inorganic hybrid sorbents based on red mud and nanosized magnetite for large scale applications in As(V) removal. *Chemical Engineering Journal*, *311*, 117–125. <https://doi.org/10.1016/j.cej.2016.11.081>
70. Lu, C., Li, L., Xu, J., Zhao, H., & Chen, M. (2024). Research on the Critical Value of Sand Permeability Particle Size and Its Permeability Law after Mixing. *Water*, *16*(3), 393. <https://doi.org/10.3390/w16030393>
71. Lu, G., Zhang, T., Zheng, C., Zhu, X., Zhang, W., & Wang, Y. (2017). The influence of the silicon saturation coefficient on a calcification-carbonation method for clean and efficient use of bauxite. *Hydrometallurgy*, *174*, 97–104. <https://doi.org/10.1016/j.hydromet.2017.07.001>
72. Lyu, F., Hu, Y., Wang, L., & Sun, W. (2021). Dealkalization processes of bauxite residue: A comprehensive review. *Journal of Hazardous Materials*, *403*, 123671. <https://doi.org/10.1016/j.jhazmat.2020.123671>
73. Ma, S., Yao, Y., Bao, P., & Guo, C. (2023). Effects of moisture content on strength and compression properties of foundation soils of cultural relics in areas flooded by the Yellow River. *Frontiers in Materials*, *10*, 1186750. <https://doi.org/10.3389/fmats.2023.1186750>
74. Maihatchi, A. A., Pons, M.-N., Ricoux, Q., Goettmann, F., & Lopicque, F. (2020). Production of electrolytic iron from red mud in alkaline media. *Journal of Environmental Management*, *266*, 110547. <https://doi.org/10.1016/j.jenvman.2020.110547>
75. Manfroi, E. P., Cheriaf, M., & Rocha, J. C. (2014). Microstructure, mineralogy and environmental evaluation of cementitious composites produced with red mud waste. *Construction and Building Materials*, *67*, 29–36. <https://doi.org/10.1016/j.conbuildmat.2013.10.031>
76. Maritsa, L., Tsakiridis, P. E., Katsiotis, N. S., Tsiaivos, H., Velissariou, D., Xenidis, A., & Beazi-Katsioti, M. (2016). Utilization of spilitic mining wastes in the construction of landfill bottom liners. *Journal of Environmental Chemical Engineering*, *4*(2), 1818–1825. <https://doi.org/10.1016/j.jece.2016.03.011>
77. Marschalko, M., Zięba, Z., Niemiec, D., Neuman, D., Mońka, J., & Dąbrowska, J. (2021). Suitability of engineering-geological environment on the basis of its permeability coefficient: four case studies of fine-grained soils. *Materials*, *14*(21), 6411. <https://doi.org/10.3390/ma14216411>
78. Mayes, W. M., Jarvis, A. P., Burke, I. T., Walton, M., Feigl, V., Klebercz, O., & Gruiz, K. (2011). Dispersal and attenuation of trace contaminants downstream of the ajka bauxite residue (red mud) depository failure, Hungary. *Environmental Science & Technology*, *45*(12), 5147–5155. <https://doi.org/10.1021/es200850y>
79. Ministry of EMR. (2016). *The Impact of Bauxite Downstreaming on the Regional Economy of West Kalimantan Province*. Center for Data and Information Technology, Ministry of Energy and Mineral Resources.
80. Ministry of Health of the Republic of Indonesia. (2023). *Regulation No. 2 of 2023 concerning the Implementation of Government Regulation No. 66 of 2014 on Environmental Health (2)*.
81. Momeni, M., Bayat, M., & Ajalloeian, R. (2022). Laboratory investigation on the effects of pH-induced changes on geotechnical characteristics of clay soil. *Geomechanics and Geoengineering*, *17*(1), 188–196. <https://doi.org/10.1080/17486025.2020.1716084>
82. Montelli, A., Gulick, S. P. S., Worthington, L. L., Mix, A., Davies-Walczak, M., Zellers, S. D., & Jaeger, J. M. (2017). Late Quaternary glacial dynamics and sedimentation variability in the Bering Trough, Gulf of Alaska. *Geology*, *45*(3), 251–254. <https://doi.org/10.1130/G38836.1>
83. Muhmed, A., Mohamed, M., & Khan, A. (2022). The Impact of Moisture and Clay Content on the Unconfined Compressive Strength of Lime Treated Highly Reactive Clays. *Geotechnical and Geological Engineering*, *40*(12), 5869–5893. <https://doi.org/10.1007/s10706-022-02255-x>
84. Mukiza, E., Zhang, L., Liu, X., & Zhang, N. (2019). Utilization of red mud in road base and subgrade materials: A review. *Resources, Conservation and Recycling*, *141*, 187–199. <https://doi.org/10.1016/j.resconrec.2018.10.031>
85. Nath, H., Kabir, M. H., Kafy, A.-A., Rahaman, Z. A., & Rahman, M. T. (2023). Geotechnical properties and applicability of bentonite-modified local soil as landfill and environmental sustainability liners. *Environmental and Sustainability Indicators*, *18*, 100241. <https://doi.org/10.1016/j.indic.2023.100241>
86. Nikbin, I. M., Aliaghazadeh, M., Sh Charkhtab, & Fathollahpour, A. (2018). Environmental impacts and mechanical properties of lightweight concrete containing bauxite residue (red mud). *Journal of Cleaner Production*, *172*, 2683–2694. <https://doi.org/10.1016/j.jclepro.2017.11.143>
87. Onyelowe, K. C., Naghizadeh, A., Aneke, F. I., Kontoni, D.-P. N., Onyia, M. E., Welman-Purchase, M., Ebid, A. M., Adah, E. I., & Stephen, L. U. (2023). Characterization of net-zero pozzolanic potential of thermally-derived metakaolin samples for sustainable carbon neutrality construction. *Scientific Reports*, *13*(1), 18901. <https://doi.org/10.1038/s41598-023-46362-y>

88. Panda, I., Jain, S., Das, S. K., & Jayabalan, R. (2017). Characterization of red mud as a structural fill and embankment material using bioremediation. *International Biodeterioration & Biodegradation*, *119*, 368–376. <https://doi.org/10.1016/j.ibiod.2016.11.026>
89. Pepper, R. A., Couperthwaite, S. J., & Millar, G. J. (2018). Re-use of waste red mud: Production of a functional iron oxide adsorbent for removal of phosphorous. *Journal of Water Process Engineering*, *25*, 138–148. <https://doi.org/10.1016/j.jwpe.2018.07.006>
90. Power, G., Gräfe, M., & Klauber, C. (2011). Bauxite residue issues: I. Current management, disposal and storage practices. *Hydrometallurgy*, *108*(1–2), 33–45. <https://doi.org/10.1016/j.hydromet.2011.02.006>
91. Purbasari, A., & Samadhi, T. W. (2021). Kajian Dehidroksilasi Termal Kaolin menjadi Metakaolin menggunakan Analisis Termogravimetri. *ALCHEMY Jurnal Penelitian Kimia*, *17*(1), 105. <https://doi.org/10.20961/alchemy.17.1.47337.105-112>
92. Ramdhani, E. P., Yulita, I., Edelwis, T. W., Permana, D., Kadir, L. A., Wahab, W., Pardi, H., Siregar, N., Santoso, E., & Prasetyoko, D. (2023). Characterisation of bauxite cleaning waste in Tanjungpinang Indonesia. *IOP Conference Series: Earth and Environmental Science*, *1148*(1), 012001. <https://doi.org/10.1088/1755-1315/1148/1/012001>
93. Rowe, R. K. (2005). Long-term performance of contaminant barrier systems. *Géotechnique*, *55*(9), 631–678. <https://doi.org/10.1680/geot.2005.55.9.631>
94. Rubinos, D. A., & Barral, M. T. (2013). Fractionation and mobility of metals in bauxite red mud. *Environmental Science and Pollution Research*, *20*(11), 7787–7802. <https://doi.org/10.1007/s11356-013-1477-4>
95. Rubinos, D. A., & Spagnoli, G. (2018). Utilization of waste products as alternative landfill liner and cover materials – A critical review. *Critical Reviews in Environmental Science and Technology*, *48*(4), 376–438. <https://doi.org/10.1080/10643389.2018.1461495>
96. Rubinos, D., Spagnoli, G., & Barral, M. T. (2015). Assessment of bauxite refining residue (red mud) as a liner for waste disposal facilities. *International Journal of Mining, Reclamation and Environment*, *29*(6), 433–452. <https://doi.org/10.1080/17480930.2013.830906>
97. Salih, Wdah. T., Yu, W., Dong, X., & Hao, W. (2020). Study on stress-strain-resistivity and microscopic mechanism of red mud waste modified by desulphurization gypsum-fly ash under drying-wetting cycles. *Construction and Building Materials*, *249*, 118772. <https://doi.org/10.1016/j.conbuildmat.2020.118772>
98. Salim, M. U., Mosaberpanah, M. A., Danish, A., Ahmad, N., Khalid, R. A., & Moro, C. (2023). Role of bauxite residue as a binding material and its effect on engineering properties of cementitious Composites: A review. *Construction and Building Materials*, *409*, 133844. <https://doi.org/10.1016/j.conbuildmat.2023.133844>
99. Samal, S. (2021). Utilization of Red Mud as a Source for Metal Ions—A Review. *Materials*, *14*(9), 2211. <https://doi.org/10.3390/ma14092211>
100. Santi, M. (2018). Netralisasi Air Lindi Residu Bauksit (Red Mud) dengan Menggunakan Air Gambut. *Jurnal Ilmiah Teknosains*, *4*(2), 76–79. <https://doi.org/10.26877/jitek.v4i2.3109>
101. Saukani, M., Sholehah, I., Arief, S., & Husein, S. (2020). Characterization of Thermal Stability of Kaolin Clay from South Kalimantan Substrate. *Jurnal Fisika Dan Aplikasinya*, *16*(1), 29. <https://doi.org/10.12962/j24604682.v16i1.4756>
102. Shi, W., Ren, H., Huang, X., Li, M., Tang, Y., & Guo, F. (2020). Low cost red mud modified graphitic carbon nitride for the removal of organic pollutants in wastewater by the synergistic effect of adsorption and photocatalysis. *Separation and Purification Technology*, *237*, 116477. <https://doi.org/10.1016/j.seppur.2019.116477>
103. Shin, W.-S., Kang, K., & Kim, Y.-K. (2014). Adsorption Characteristics of Multi-Metal Ions by Red Mud, Zeolite, Limestone, and Oyster Shell. *Environmental Engineering Research*, *19*(1), 15–22. <https://doi.org/10.4491/eer.2014.19.1.015>
104. Shu, S., Zhu, W., & Shi, J. (2019). A new simplified method to calculate breakthrough time of municipal solid waste landfill liners. *Journal of Cleaner Production*, *219*, 649–654. <https://doi.org/10.1016/j.jclepro.2019.02.050>
105. Silva, S. H. G., Hartemink, A. E., Teixeira, A. F. D. S., Inda, A. V., Guilherme, L. R. G., & Curi, N. (2018). Soil weathering analysis using a portable X-ray fluorescence (PXRF) spectrometer in an Inceptisol from the Brazilian Cerrado. *Applied Clay Science*, *162*, 27–37. <https://doi.org/10.1016/j.clay.2018.05.028>
106. Simon, A., Wilhelmy, M., Klosterhuber, R., Cocuzza, E., Geitner, C., & Katzensteiner, K. (2021). A system for classifying subsolum geological substrates as a basis for describing soil formation. *CATENA*, *198*, 105026. <https://doi.org/10.1016/j.catena.2020.105026>
107. Skempton, A. W. (1953). *The colloidal activity of clay*, *Proceedings of the Third International Conference on Soil Mechanics and Foundation Engineering*, *1*, 57–61.
108. Stenchly, K., Dao, J., Lompo, D. J.-P., & Buerkert, A. (2017). Effects of waste water irrigation on soil properties and soil fauna of spinach fields in a West African urban vegetable production system. *Environmental Pollution*, *222*, 58–63. <https://doi.org/10.1016/j.envpol.2017.01.006>



109. Sun, H., Chen, C., Ling, L., Memon, S. A., Ding, Z., Li, W., Tang, L., & Xing, F. (2019). Synthesis and Properties of Red Mud-Based Nanoferrite Clinker. *Journal of Nanomaterials*, 2019, 1–12. <https://doi.org/10.1155/2019/3617050>
110. Surbakti, R. (2021). Analisis Penurunan Tanah dengan Plaxis 2D dan 3D Pada Proyek Reklamasi Belawan. *Syntax Literate ; Jurnal Ilmiah Indonesia*, 6(7), 3511. <https://doi.org/10.36418/syntax-literate.v6i7.1532>
111. Tabereaux, A. T., & Peterson, R. D. (2014). Aluminum Production. In *Treatise on Process Metallurgy* (pp. 839–917). Elsevier. <https://doi.org/10.1016/B978-0-08-096988-6.00023-7>
112. USEPA. (1992a). *SW-846 Method 1311: Toxicity Characteristic Leaching Procedure*. United States Environmental Protection Agency. <https://www.epa.gov/hw-sw846/sw-846-test-method-1311-toxicity-characteristic-leaching-procedure>
113. USEPA. (1992b). *The Environmental Protection Agency's Municipal Solid Waste Landfill Liner Design Criteria*.
114. Viyasun, K., Anuradha, R., Thangapandi, K., Santhosh Kumar, D., Sivakrishna, A., & Gobinath, R. (2021). Investigation on performance of red mud based concrete. *Materials Today: Proceedings*, 39, 796–799. <https://doi.org/10.1016/j.matpr.2020.09.637>
115. Waluyo, J., Amal, R. R. I., Yudistira, A. A., Mustofa, H., & Maulana, M. L. (2022). Influence of Fly Ash as a Catalyst on the Pyrolysis Process of Rice Husk Pellets towards Thermal Characteristics and Synthetic Gas (Syngas) Production. *ALCHEMY Jurnal Penelitian Kimia*, 18(2), 148. <https://doi.org/10.20961/alchemy.18.2.55193.148-157>
116. Wan, Y., Dong, Z., Cai, Y., Xue, Q., Liu, K., Liu, L., & Guo, D. (2023). Geomembrane leaks detection and leakage correlation factor analysis of composite liner systems for fifty-five (55) solid waste landfills in China. *Environmental Technology & Innovation*, 32, 103308. <https://doi.org/10.1016/j.eti.2023.103308>
117. Wang, H., Liu, Z., Xie, Y., & Li, Y. (2024). Study on the Influence of Moisture Content and Void Ratio on the Disintegration of Red Clay. *Applied Sciences*, 14(9), 3652. <https://doi.org/10.3390/app14093652>
118. Wang, L., Sun, N., Tang, H., & Sun, W. (2019). A Review on Comprehensive Utilization of Red Mud and Prospect Analysis. *Minerals*, 9(6), 362. <https://doi.org/10.3390/min9060362>
119. Wang, P., & Liu, D.-Y. (2012). Physical and Chemical Properties of Sintering Red Mud and Bayer Red Mud and the Implications for Beneficial Utilization. *Materials*, 5(10), 1800–1810. <https://doi.org/10.3390/ma5101800>
120. Wang, Q., Ji, C., Sun, J., Yao, Q., Liu, J., Saeed, R. M. Y., & Zhu, Q. (2020). Kinetic thermal behavior of nanocellulose filled polylactic acid filament for fused filament fabrication 3D printing. *Journal of Applied Polymer Science*, 137(7), 48374. <https://doi.org/10.1002/app.48374>
121. Wang, S., Jin, H., Deng, Y., & Xiao, Y. (2021). Comprehensive utilization status of red mud in China: A critical review. *Journal of Cleaner Production*, 289, 125136. <https://doi.org/10.1016/j.jclepro.2020.125136>
122. Wang, X., Sun, T., Kou, J., Li, Z., & Tian, Y. (2018). Feasibility of co-reduction roasting of a saprolitic laterite ore and waste red mud. *International Journal of Minerals, Metallurgy, and Materials*, 25(6), 591–597. <https://doi.org/10.1007/s12613-018-1606-7>
123. Wang, Y., Zhang, S., Yin, S., Liu, X., & Zhang, X. (2020). Accumulated plastic strain behavior of granite residual soil under cycle loading. *International Journal of Geomechanics*, 20(11), 04020205. [https://doi.org/10.1061/\(ASCE\)GM.1943-5622.0001850](https://doi.org/10.1061/(ASCE)GM.1943-5622.0001850)
124. Wibawa, Y. S., Sugiarti, K., & Soebowo, E. (2018). Characteristics and engineering properties of residual soil of volcanic deposits. *IOP Conference Series: Earth and Environmental Science*, 118, 012041. <https://doi.org/10.1088/1755-1315/118/1/012041>
125. Winkler, D. (2014). Collembolan response to red mud pollution in Western Hungary. *Applied Soil Ecology*, 83, 219–229. <https://doi.org/10.1016/j.apsoil.2013.07.006>
126. Wu, C., & Liu, D. (2012). Mineral Phase and physical properties of red mud calcined at different temperatures. *Journal of Nanomaterials*, 2012, 1–6. <https://doi.org/10.1155/2012/628592>
127. Wulandari, P. S., & Tjandra, D. (2019). Analysis of the effect of reservoir water level fluctuations on reservoir slope stability using the 2D plaxis program. *MEDIA KOMUNIKASI TEKNIK SIPIL*, 24(2), 113. <https://doi.org/10.14710/mkts.v24i2.17780>
128. Yao, F., Xu, P., Jia, H., Li, X., Yu, H., & Li, X. (2022). Thermogravimetric Analysis on a Resonant Microcantilever. *Analytical Chemistry*, 94(26), 9380–9388. <https://doi.org/10.1021/acs.analchem.2c01374>
129. Yeom, C., & Kim, Y. (2017). Adsorption of ammonia using mesoporous alumina prepared by a templating method. *Environmental Engineering Research*, 22(4), 401–406. <https://doi.org/10.4491/eer.2017.045>
130. Zhang, D.-R., Chen, H.-R., Zhao, X.-J., Xia, J.-L., Nie, Z., Zhang, R., Shu, W.-S., & Pakostova, E. (2022). Fe(II) bio-oxidation mediates red mud transformations to form Fe(III)/Al (hydr)oxide

- adsorbent for efficient As(V) removal under acidic conditions. *Chemical Engineering Journal*, 439, 135753. <https://doi.org/10.1016/j.cej.2022.135753>
131. Zhang, H., Cao, T., Sun, X., & Xu, Y. (2021). Temporal and spatial variation characteristics of soil mechanical composition after aeolian soil improvement by soft rock in Mu Us sandy land. *Bangladesh Journal of Botany*, 865–872. <https://doi.org/10.3329/bjb.v50i5.56438>
132. Zhang, J., Liu, S., Yao, Z., Wu, S., Jiang, H., Liang, M., & Qiao, Y. (2018). Environmental aspects and pavement properties of red mud waste as the replacement of mineral filler in asphalt mixture. *Construction and Building Materials*, 180, 605–613. <https://doi.org/10.1016/j.conbuildmat.2018.05.268>
133. Zhang, S., Yang, J., Xin, X., Yan, L., Wei, Q., & Du, B. (2015). Adsorptive removal of Cr(VI) from aqueous solution onto different kinds of modified bentonites. *Environmental Progress & Sustainable Energy*, 34(1), 39–46. <https://doi.org/10.1002/ep.11947>
134. Zhang, S.-C., Li, K., Sun, K.-M., & Wang, S. (2022). Impact of Initial Moisture Content on the Shrinkage-Swelling Behavior of Heishan Bentonite. *KSCE Journal of Civil Engineering*, 26(2), 550–555. <https://doi.org/10.1007/s12205-021-0060-7>
135. Zhang, Y., Qian, W., Zhou, P., Liu, Y., Lei, X., Li, B., & Ning, P. (2021). Research on red mud-limestone modified desulfurization mechanism and engineering application. *Separation and Purification Technology*, 272, 118867. <https://doi.org/10.1016/j.seppur.2021.118867>
136. Zhang, Z., Huang, X., Liu, W., & Wang, L. (2020). Study on the Hydraulic Parameters of Woshaxi Landslide Soils during Water Level Drawdown of Three Gorges Reservoir. *Geofluids*, 2020, 1–14. <https://doi.org/10.1155/2020/6283791>
137. Zhang, Z., Zhou, D., He, J., He, Y., Yu, C., Long, Y., Shen, D., Yao, J., & Chen, H. (2023). Insight into the impact of industrial waste co-disposal with MSW on groundwater contamination at the open solid waste dumping sites. *Chemosphere*, 344, 140429. <https://doi.org/10.1016/j.chemosphere.2023.140429>
138. Zhou, R., Liu, X., Luo, L., Zhou, Y., Wei, J., Chen, A., Tang, L., Wu, H., Deng, Y., Zhang, F., & Wang, Y. (2017). Remediation of Cu, Pb, Zn and Cd-contaminated agricultural soil using a combined red mud and compost amendment. *International Biodeterioration & Biodegradation*, 118, 73–81. <https://doi.org/10.1016/j.ibiod.2017.01.023>